doi:10.1093/brain/awn005 *Brain* (2008), **131**, 1113–1122

Thrombin receptor PAR-1 on myelin at the node of Ranvier: a new anatomy and physiology of conduction block

Efrat Shavit,[1,*] Orit Beilin,[1,*] Amos D. Korczyn,[1,2,3] Constantin Sylantiev,[2] Ramona Aronovich,[1] Vivian E. Drory,[2] David Gurwitz,[4] Ido Horresh,[5] Rachel Bar-Shavit,[6] Elior Peles[5] and Joab Chapman[1,2]

[1]Department of Physiology and Pharmacology, [2]Department of Neurology, [3]Sieratzki Chair of Neurology, [4]Department of Human Genetics and Molecular Medicine, Sackler Faculty of Medicine, Tel Aviv University, Tel Aviv 69978, [5]Department of Molecular Cell Biology, Weizmann Institute for Scientific Research, Rehovot and [6]Department of Oncology, Hadassah-Hebrew University Hospital, Jerusalem, Israel

*These authors contributed equally to this work.

Correspondence to: Professor Joab Chapman, Department of Physiology and Pharmacology, Sackler Faculty of Medicine, Tel Aviv University, Ramat Aviv 69978, Israel
E-mail: jchapman@post.tau.ac.il

Inflammatory demyelinating diseases of peripheral nerves are associated with altered nerve conduction and with activation of the coagulation pathway. Thrombin mediates many of its effects through protease-activated receptor 1 (PAR-1). We examined the possibility that thrombin may mediate conduction abnormalities through PAR-1 on rat sciatic nerve. PAR-1 was found to be present by both RT-PCR and Western blot analysis of the sciatic nerve. Activation of PAR-1 by a specific peptide agonist caused a 3-fold increase in phosphorylated extracellular signal-regulated kinase (ERK) in the sciatic nerve indicating the existence of functional receptors in the nerve. By confocal immunofluoresence microscopy of the sciatic nerve using anti-PAR-1 antibody and double staining for the paranodal marker contactin-associated protein 1 (Caspr1) or the nodal markers gliomedin and ezrin, the receptor was localized predominantly to myelin microvilli at the node of Ranvier. Thrombin and the PAR-1-specific agonist were applied to exposed rat sciatic nerve and their effects on nerve conduction were measured. Thrombin at concentrations of 100 and 200 U/ml and PAR-1 agonists 150 and 300 μM produced a conduction block within 30 min of application. This effect was maintained for at least 1 h and was reversible by washing. The function of the nodal non-compacted myelin is not well known. The current results implicate this structure and PAR-1 activation in the pathogenesis of conduction block in inflammatory and thrombotic nerve diseases.

Keywords: protease activated receptors; thrombin; node of Ranvier; conduction block

Abbreviations: BBB = blood–brain barrier; BNB = blood–nerve barrier; CNS = central nervous system; DRG = dorsal root ganglia; EAN = experimental autoimmune neuritis; GBS = Guillain–Barre syndrome; PNS = peripheral nervous system

Received April 26, 2007. Revised December 29, 2007. Accepted January 8, 2008. Advance Access publication February 25, 2008

Many inflammatory diseases of the peripheral and central nervous systems (PNS and CNS) have a predilection for myelin and affect conduction in nerves and CNS tracts. In the PNS the prototypical inflammatory disease affecting nerves is the Guillain–Barre syndrome (GBS) and its animal model, experimental autoimmune neuritis (EAN). In these diseases an early (Ropper *et al.*, 1990) and often reversible (Berger *et al.*, 1988) block in the conduction of action potentials along myelinated axons is a key feature (Turnell *et al.*, 1995). The specific pathogenesis of this conduction block is not fully understood (Hughes *et al.*, 1999). While some investigators have suggested that local effects of autoantibodies from GBS patients and especially antibodies to gangliosides may directly bind to the nodes of Ranvier and affect conduction of action potentials, such findings have not been confirmed by other well-performed studies (Harvey *et al.*, 1995; Hirota *et al.*, 1997; Hughes *et al.*, 1999; Paparounas *et al.*, 1999). Alternative factors

© The Author (2008). Published by Oxford University Press on behalf of the Guarantors of Brain. All rights reserved. For Permissions, please email: journals.permissions@oxfordjournals.org

Downloaded from brain.oxfordjournals.org at Wix Library on July 31, 2011

such as secreted peptides have been implicated in causing nerve conduction block (Brinkmeier *et al.*, 2000)

There is growing evidence that links inflammation and the coagulation system (Cicala and Cirino, 1998; Esmon, 2001). Previous studies demonstrate activation of the coagulation system in experimental autoimmune encephalomyelitis (EAE): permeabilization of the blood–brain barrier (BBB) is associated with CNS perivascular fibrin deposition (Koh *et al.*, 1992) and levels of plasma thrombin–antithrombin III complexes are elevated in EAE rats (Inaba *et al.*, 2001). We have found high levels of thrombin inhibitors both early in its course and at the peak of the disease (Beilin *et al.*, 2005). These findings imply that neuronal tissue may be exposed to high levels of thrombin during inflammatory demyelinating diseases.

Thrombin, a multifunctional serine protease, is a key enzyme in the coagulation cascade formed after cleavage of its precursor, prothrombin, by the coagulation factor Xa. In addition to its role in thrombogenesis, thrombin has hormone-like activities and is known to affect various cells such as platelets, T cells and, in the CNS, microglia, neurons and astrocytes (Bar-Shavit *et al.*, 1986; Coughlin, 2000). In the brain thrombin has mitogenic effects on astrocytes, fibroblasts and smooth muscle cells, regulates astrocyte stellation and induces neurite retraction (Gurwitz and Cunningham, 1988; Cunningham and Donovan, 1997). Most of these effects are mediated by the G protein-coupled protease activated receptor (PAR) group of proteins (Schmidlin and Bunnett, 2001). PAR-1 is activated by thrombin while PAR-2 is activated by trypsin or tryptase. PAR-1 is expressed in a variety of tissues including platelets, endothelial cells, smooth muscle, T cells, mast cells, glial cells and neurons (Dery *et al.*, 1998). Thrombin cleaves this receptor at the extracellular domain to form a new NH_2-terminal tethered ligand with the sequence SFLLRN (Vu *et al.*, 1991). It has therefore become possible to synthesize peptides which mimic the action of the tethered ligand and are specific pharmacological agonists of PAR-1.

In the PNS studies have demonstrated the deleterious effects of thrombin on sciatic regeneration (Friedmann *et al.*, 1999). Recent studies suggest that thrombin through PARs has a direct physiological effect on neuronal function in sensory pathways (Steinhoff *et al.*, 2003; Vergnolle *et al.*, 2003; Kawao *et al.*, 2004; Narita *et al.*, 2005) and in the retina (Luo *et al.*, 2005). It has been previously shown that PAR-1 is expressed in spinal motor neurons and that its over-expression is linked to their degeneration (Festoff *et al.*, 2000). It is not known whether, in addition to axons of motor neurons, PAR-1 is expressed in non-neuronal sciatic tissue such as Schwann cells nor if it exerts effects that contribute to nerve dysfunction. In the present study we found that functional PAR-1 receptors exist specifically in the non-compacted Schwann cell myelin microvilli at the nodes of Ranvier in the sciatic nerve. Electrophysiological experiments demonstrated that PAR-1 activation results in conduction block in motor fibres.

Materials and Methods

Animals

Adult male Wistar rats weighing 300–400 g were used for all experiments. The animals used in this study were cared for in accordance to the guidelines published in the National Institutes of Health *Guide for the Care and Use of Laboratory Animals* (Clark, 1996), and the study was approved by the Animal Welfare Committee of Sackler Faculty of Medicine. Rats were anaesthetized by intraperitoneal (IP) injections of Equitezin (4% chloral hydrate, 6% sodium pentobarbital) 0.5 ml/100 g body weight, 15–20 min before the removal of the nerves or the electrophysiological procedure.

RT-PCR for rat PAR-1

Total RNA was isolated from rat sciatic and optic nerves using RNeasy lipid tissue kit (QIAGEN, Hilden, Germany). The amount of total RNA was determined by measuring its absorption at 260 nm in Gene Quant (Pharmacia Biotech). Two hundred nanograms of RNA was used for complementary DNA (cDNA) synthesis, employing Revers-IT synthesis kit (ABgene, Epsom, UK). PAR-1 transcript was amplified, using Reddymix (ABgene, Epsom, UK) for 25 µl total PCR reaction; 95°C for 3 min for initial melting was followed by 23–29 cycles of 95°C for 45 s, 57°C for 30 s and 72°C for 30 s; 5 min at 72°C was used for final extension after cycling. PCR primers were as follows: upstream 5′-GCCTCCATCATGCTCATGAC-3′ downstream 5′-AAAGCAGA CGATGAAGATGCA-3′. Primers for gliomedin and actin were as previously described (Spiegel *et al.*, 2007).

Western blot analysis of PAR-1 in sciatic nerve

Sciatic nerves were isolated from normal rats and washed with ice-cold phosphate-buffered saline (PBS). The epineurium was gently rolled-up and the fibres were homogenized using a Teflon pestle. Proteins from the sciatic homogenates (25 µg total protein) were separated by polyacrylamide gel electrophoresis and transferred onto nitrocellulose membranes for Western blot analysis (Towbin *et al.*, 1979). Membranes were incubated with primary rabbit anti PAR-1 antibody (diluted 1/500, ABCAM-ab32611) at room temperature for 1.5 h. As a control, the primary antibody was incubated prior to use, with the peptide used to generate it, SFLLRNPNDKYEPF (Bachem, H-8105) overnight with gentle agitation at 4°C. Positive controls were human platelets and negative controls were rat platelets known not to contain PAR-1. Membranes were incubated at room temperature with horseradish peroxidase-conjugated goat anti-rabbit antibody (Jackson Immunoresearch Laboratories) and bound antibody detected using enhanced chemiluminescence (ECL) assay kit (Pierce).

Determination of extracellular signal-regulated kinase (ERK) phosphorylation

Sciatic nerves were dissected into 20–30 mm long 100 mg sections each placed individually in 24-well plates and incubated for 2 h at 37°C in media consisting of Ham's F-10 medium containing 5% foetal calf serum (FCS), penicillin (100 mg/ml), G-418 (400 µg/ml), streptomycin (100 mg/ml) and L-glutamine (2 mM). Saline, thrombin (0.1 U/ml) or the PAR-1-specific agonist SFLLRNPNDKYEPF (10 µM) were added to the nerves for 7 min, at 37°C. ERK phosphorylation was then detected in the nerve homogenates: Medium was aspirated and to each well we

Downloaded from brain.oxfordjournals.org at Wix Library on July 31, 2011

added 0.5 ml of solubilization buffer [50 mM HEPES, 50 mM NaCl, 1 mM ethylene glycol-*bis*(2-aminoethyl)-tetraacetic acid (EGTA), 10% glycerol, 1% Triton X-100, 1.5 mM $MgCl_2$], and the plate was kept on ice for 10 min. The contents of each well were homogenized, collected into Eppendorf tubes and centrifuged at 14 000 rpm for 10 min at 4°C. The supernatants were collected and placed immediately on ice and 10 µg protein from each were separated by SDS–polyacrylamide gel electrophoresis [10% acrylamide (Laemmli, 1970)]. The proteins were then transferred onto nitrocellulose filters (Towbin *et al.*, 1979). Membranes were incubated with mouse anti phosphorylated-ERK 1,2 (diluted 1/10 000, Sigma) at room temperature for 2 h and washed. Membranes were then incubated at room temperature with horseradish peroxidase-conjugated goat anti-mouse antibody. Protein bands were detected by a peroxidase-based ECL method with luminol.

Immunohistological localization of PAR-1 on teased sciatic nerve fibres

Sciatic nerves were isolated from normal rats and fixed for 10 min in Zamboni's fixative, washed in PBS, and teased into single fibres on Superfrost Plus slides (Fisher). The fibres were then permeabilized for 10 min in cold methanol at –20°C. Slides were then washed with PBS, blocked for 1 h in PBS containing 1% goat serum, 0.2% glycine and 0.1% Triton X-100, and incubated overnight with rabbit polyclonal anti PAR-1 antibody (1:50) or control antibodies which included mouse monoclonal antibodies against Caspr, gliomedin both 1:1000 (Poliak *et al.*, 1999; Eshed *et al.*, 2005), Ezrin 1:500 (clone 3C12; Sigma, St Louis, MO), panNav channels (sodium channels) K58/35-1; 1:50 (Rasband *et al.*, 1999), myelin-associated glycoprotein (MAG) Clone 513, 1:300, polyclonal rat anti-Caspr (1:500; prepared by injection of GST fusion Caspr C-terminus). After subsequent washes in PBS, the slides were reacted with RRX- or Cy2-coupled secondary antibodies obtained from Jackson Immunoresearch Laboratories. Immunofluorescence slides were viewed and analysed using a confocal microscope ZEISS, CLSM 410.

Electrophysiological studies

The sciatic nerve was exposed by an anterior approach to the proximal part of the nerve (above its bifurcation to the common peroneal and tibial nerves) and a chamber formed between the muscles surrounding the nerve which was completely filled with 20 µl of solution. The length of the exposed nerve was 10 mm. The test substance was in contact with surrounding muscle but not with the plantar muscle in which the motor response was monitored. The 200 µl volume was applied in 20 µl aliquots every 5 min in order to compensate for diffusion and drying of the solution. Reversal of the pharmacological effects was studied by applying 50 µl of saline to the nerve every 3 min and excess liquid was gently absorbed each time just before the application of the next solution. The excess solution was absorbed just before neurographic motor response recordings were performed at 30 and 60 min after the first application of the solution. A bipolar electrode was placed under the proximal part of the sciatic nerve or inserted distally to the chamber and the nerve stimulated using single square waves of 0.25 ms duration at supramaximal intensity (Grass medical instruments stimulator model SD9). The compound muscle action potentials (CMAPs) were recorded by ring surface electrodes applied around the plantar muscle. The EMG responses were displayed on a Tektronix dual beam storage oscilloscope (Tektronix, Beaverton, Oregon) and recorded by camera (Model DS-34, Polaroid, Cambridge, Massachusetts) for further analysis. In later experiments a fully digital recording Keypoint apparatus was used (Dantec, Skovlunde, Denmark). Latency was measured as the time interval from the stimulus artifact to the first deflection from baseline. Amplitude of the CMAP was measured from the negative to the positive peaks (peak-to-peak amplitude). The change of CMAP induced by the drug was calculated by the equation $CMAP_t/CMAP_0 \times 100$ where $CMAP_0$ was recorded just before applying the substance and $CMAP_t$ was recorded t minutes after application. All the results presented are from procedures performed with the experimenter blinded to the content of the solutions applied to the nerve. In the electrophysiology experiments temperature was maintained by performing the experiments under a warming lamp by which body temperature is maintained between 34.8 and 36.9°C (Kafri *et al.*, 2002).

Substances applied to the nerve

Physiological saline (NaCl 0.9%) was used as a control solution. Thrombin and the PAR-1 agonist SFLLRNPNDKYEPF were obtained from Sigma (T4648 and T1063, St Louis, Missouri) and the shorter PAR-1 agonist (SFLLRN-amide) from Bachem (Bubendorf, Switzerland). The PAR-1 antagonist, SCH 79797 dihydrochloride (1 µM) obtained from Tocris Bioscience (Ellisville, Missouri), was mixed with the PAR-1 agonist (SFLLRN-amide 150 µM) and the solution was then applied to the nerve. The thrombin inhibitor, Phe-Pro-Arg-chloromethylketone (PPACK, 500 µM) obtained from Calbiochem (La Jolla, California), was mixed with thrombin (100 U/ml) and the solution was then applied to the nerve. Trypsin was purchased from Biological Industries (Beit Haemek, Israel).

Statistics

All treatments were compared to controls by means of analysis of variance (ANOVA) with repeated measures, LSD *post hoc* analysis and Student's *t*-test using SPSS software (Chicago, IL, USA).

Results

RT-PCR analysis of PAR-1 expression in teased sciatic nerve fibres pooled from two animals showed a clear signal comparable with expression of PAR-1 mRNA in the optic nerve (Fig. 1A). In Fig. 1B the expression of PAR-1 mRNA in the sciatic is compared with its expression in rat liver, brain, spinal cord and Schwann cell and dorsal root ganglia primary cultures. As can be seen, PAR-1 mRNA levels are similar in the sciatic nerve and Schwann cell culture and both samples have detectable levels of the Schwann cell marker gliomedin which is not present in the other samples. Somewhat higher levels of PAR-1 expression are seen in the brain, spinal cord and dorsal root ganglia cells. The presence of PAR-1 in the sciatic nerve was confirmed by Western blot analysis (Fig. 1C) utilizing specific antibodies. As can be seen, a major band corresponding to the expected molecular 50 kDa weight of the receptor is present in the sciatic nerve and in the positive control

Downloaded from brain.oxfordjournals.org at Wix Library on July 31, 2011

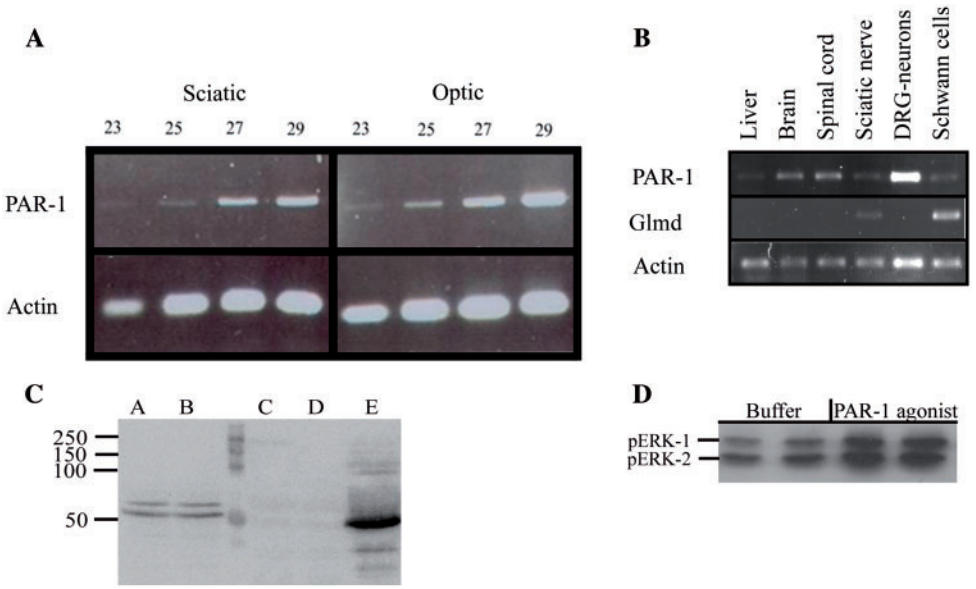

Fig. 1 Expression and activation of PAR-1 in rat sciatic nerve. **(A)** RT-PCR analyses of PAR-1 mRNA. Total RNA samples isolated from rat optic and desheathed sciatic nerve and were tested for the expression of PAR-1 and actin. Optic: optic nerve, Sciatic: Sciatic nerve. The number of PCR cycles (23–29) is indicated. **(B)** Comparison by RT-PCR (27 cycles) of PAR-1, gliomedin and actin expression in rat liver, brain, spinal cord, sciatic, DRG and Schwann cells were performed as described in the 'Methods' section. **(C)** Western blot analysis of PAR-1 immunoreactivity in desheathed rat sciatic nerve (lanes A and B), rat platelets (lanes C and D) and human platelets (lane E) was measured as described in the 'Methods' section. Molecular weight markers are represented on the left. **(D)** Induction of elevated phosphorylated ERK (pERK) levels by PAR-1 activation in the rat sciatic nerve. Western blot analysis of pERK levels in sciatic nerve homogenates after 7 min exposure to: NaCl 0.9% and SFLLRNPNDKYEPF (10 μM) was performed as described in the 'Methods' section. The anti-MAP kinase antibody reacts with pERK-1 and pERK-2 42 and 44 kDa bands, respectively.

human platelets but not in rat platelets which serve as a negative control since they are known not to contain PAR-1. Interestingly an additional major band of 58 kDa is seen in the sciatic nerve but not in the platelets which most probably represents a modified form of PAR-1. Binding of the anti-PAR-1 antibodies to both bands was completely inhibited by addition of the specific blocking peptide SFLLRNPNDKYEPF (not shown). The presence of a functional PAR-1 on the sciatic nerve was further verified by stimulating the receptor and measuring phosphorylation of ERK (pERK). Stimulation of isolated sciatic nerve by both thrombin and the PAR-1 agonist induced significant (>3-fold) increase in the levels of pERK. Figure 1D is a representative immunoblot showing the effect of the PAR-1 agonist compared to buffer alone on pERK levels in isolated rat sciatic nerve.

The specific localization of PAR-1 in teased fibres from the sciatic nerve was examined by immunofluorescence histology utilizing double and triple staining for PAR-1 together with specific markers of the node of Ranvier including the paranodal axonal marker Caspr, the glial nodal markers gliomedin and ezrin, the non-compacted myelin marker myelin associated glycoprotein (MAG), and the sodium channel nodal axonal marker (Fig. 2). Figure 2A presents typical PAR-1 staining of teased nerve fibres. As can be seen, all of nodes of Ranvier demarcated by the paranodal Caspr stains (Fig. 2B) are stained by PAR-1 (merged Fig. 2C) in a pattern that seems mainly nodal, placed just between the two paranodal axonal Caspr stained regions. Similar staining for PAR-1 was present in 49/50 nodes of Ranvier examined randomly in teased fibres. Examination of a number of higher magnification detailed images of the staining pattern for PAR-1 relative to Caspr at the node of Ranvier (Fig. 2D–F) suggested non-axonal localization on the non-compacted Schwann cell microvilli that fill the nodal gap. This was confirmed by co-staining for gliomedin which is a marker of the nodal axoglial contact site marking both glial and axonal components of the node and which showed excellent co-localization with PAR-1. In order to differentiate axonal from glial elements we searched for nodes in which mechanical movement of the axon has occurred, separating the gliomedin immunoreactivity into axonal-attached and glial components (Fig. 2H). Co-staining of such nodes for PAR-1 (Fig. 2G) demonstrates that it exclusively co-stains with the gliomedin on the Schwann cell microvilli and not on the nodal axon (Fig. 2I). In order to confirm this localization of PAR-1 we performed similar co-staining experiments with the glial nodal marker ezrin. As can be seen the staining with PAR-1 (Fig. 2J) and ezrin (Fig. 2K) were highly co-localized as shown by the yellow staining in Fig. 2L. Staining for PAR-1 (Fig. 2M) and MAG, a marker of paranodal and Schmidt–Lanterman incisures non-compacted myelin (Fig. 2N), did not show any significant co-localization as seen in Fig. 2O. Visualization of nodes in which mechanical movement of the axon had occurred

Downloaded from brain.oxfordjournals.org at Wix Library on July 31, 2011

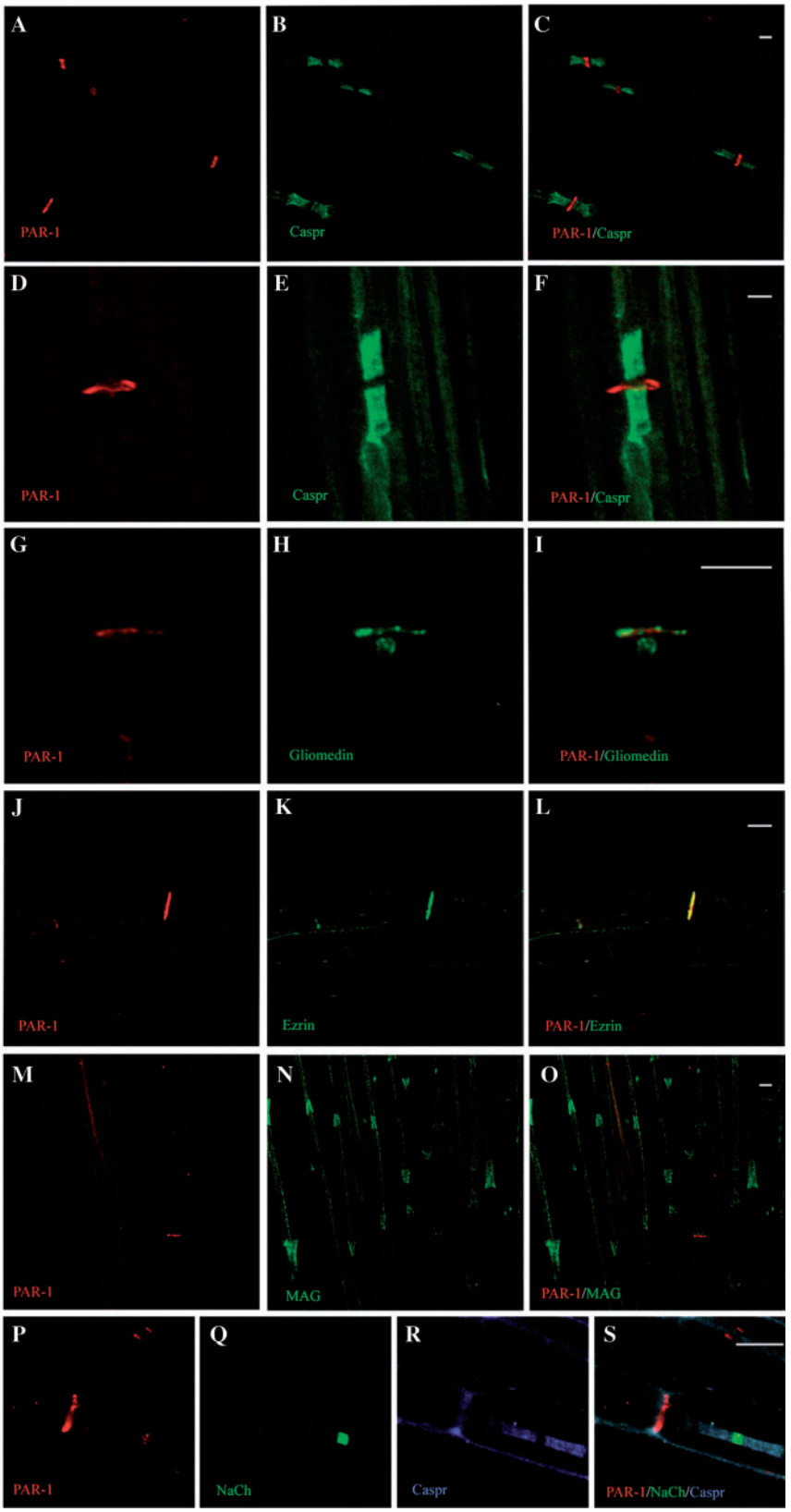

Fig. 2 PAR-1 localized to the node of Ranvier. Teased rat sciatic fibres were stained for PAR-1 (**A, D, G, J, M, P**), Caspr (**B, E, R**), gliomedin (**H**), ezrin (**K**), MAG (**N**) and sodium channel (NaCh, **Q**) and double and triple staining pictures were merged (**C, F, I, L, O, S**) as described in the 'Methods'. Bars represent 5 μm.

Downloaded from brain.oxfordjournals.org at Wix Library on July 31, 2011

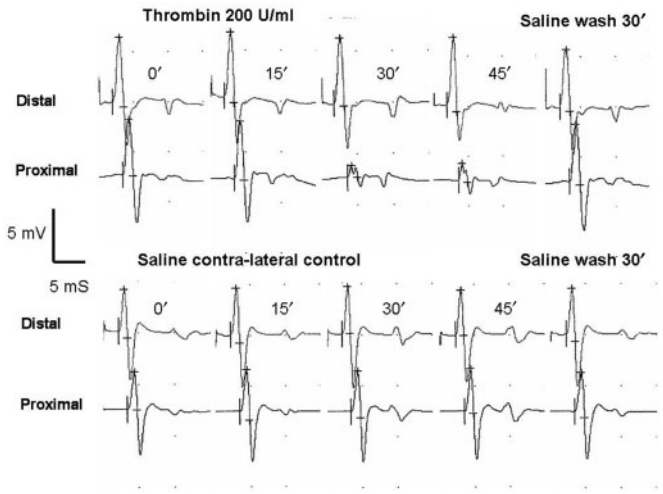

Fig. 3 Focal conduction block induced by thrombin on sciatic nerve. Muscle responses to stimulation of the nerve distal and proximal to the application of thrombin (200 U/ml) measured just before application (0′) and 15, 30 and 45 min after application (15′, 30′ and 45′) as described in the 'Methods' show a significant conduction block beginning at 30 min. The restoration of the CMAP response to proximal stimulation after 30 min saline wash is demonstrated in the far upper right corner of the figure. A control set of measurements from the contra-lateral sciatic nerve treated in parallel with saline shows no significant changes in CMAP responses to distal and proximal stimulation at any time point.

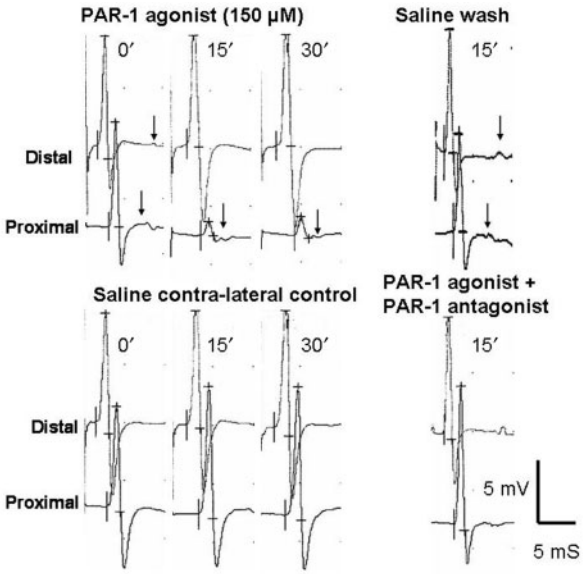

Fig. 4 The conduction block distal to the point of PAR-1 activation is reversible and blocked by a PAR-1 agonist. Muscle responses to stimulation of the nerve distal and proximal to the application of the PAR-1 agonist SFLLRN-amide measured just before application (0′) and 15 and 30 min after application (15′ and 30′) as described in the 'Methods' show a significant conduction block which is reversed by washing for 15 min with saline (saline wash). A control set of measurements from the contra-lateral sciatic nerve treated in parallel with saline shows no significant changes in CMAP responses to distal and proximal stimulation at any time point. When the PAR-1 agonist and antagonist were then applied together to this nerve for 15 min no conduction block was found. Arrows indicate F wave responses which seem more affected in response to distal stimulation.

confirmed that PAR-1 staining (Fig. 2P) did not co-localize with axonal markers such as the nodal sodium channel (Fig. 2Q) or the paranodal Caspr (Fig. 2R) as seen in the merged Fig. 2S.

Representative results of experiments in which thrombin (200 U/ml) was applied to the nerve and responses measured from the muscle following stimulation of the nerve proximally and distally to the point of application, are presented in Fig. 3. As can be seen after 30 min, treatment with thrombin caused a significant reduction in the CMAP in response to stimulation proximal but not distal to the point of application. The full restoration of the CMAP response to proximal stimulation after 30 min saline wash is demonstrated in the far upper right corner of the figure. In this set of experiments the second sciatic nerve was treated with saline in parallel and no significant changes in CMAP responses to distal and proximal stimulation were seen at any time point (Fig. 3 lower pane). In the three experiments performed in the same manner as that presented in Fig. 3, the mean (±SD) CMAP response to proximal stimulation after 30 min exposure to 200 U/ml of thrombin was 32 ± 14% of the initial (time 0) response. After 1 h of exposure to thrombin the nerves were washed for 30 min and the response to proximal stimulation recovered to 111 ± 17% of the initial response.

Figure 4 shows representative results of experiments in which the PAR-1 agoinst (SFLLRN-amide) was applied to the nerve and responses measured from the muscle following stimulation of the nerve proximally and distally to the point of application. As can be seen, the response to proximal stimulation of the nerve was significantly lower than the response to the distal stimulation and this effect was seen earlier (15 min) than with thrombin (30 min). Washing the nerve with control solution completely restored the CMAP (Fig. 4) indicating that the PAR-1 agonist effect was reversible. In four experiments performed as that presented in Fig. 4, the mean CMAP response to proximal stimulation after 30 min exposure to 150 μM of the PAR-1 agonist was 25 ± 14% of the initial (time 0) response. After 1 h of exposure to the agonist the nerves were washed for 30 min and the response to proximal stimulation recovered to 114 ± 32% of the initial response. In this set of experiments the second sciatic nerve was treated with saline in parallel and no significant changes in CMAP responses to distal and proximal stimulation were seen at any time point (Fig. 4). Application of the specific PAR-1 antagonist SCH 79797 completely blocked the effect of the PAR-1 agonist on nerve conduction (Fig. 4). Thrombin prolonged distal latency by 10% after 30 min (112 ± 9%, NS) and by 20% (121 ± 7% $P = 0.016$ by Student's *t*-test) 60 min after the application.

A quantitative summary of similar studies using three different doses of thrombin (three preparations each)

Downloaded from brain.oxfordjournals.org at Wix Library on July 31, 2011

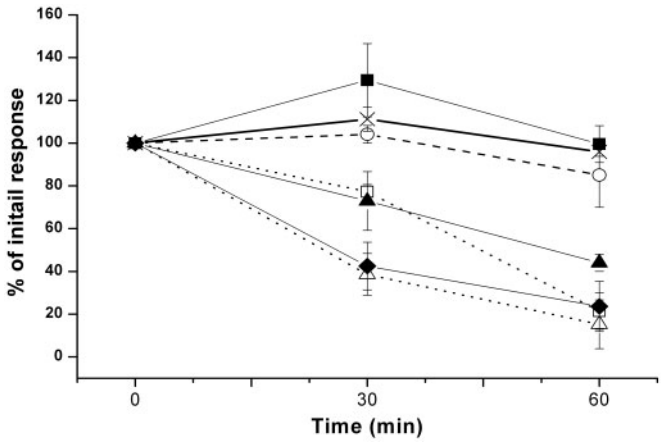

Fig. 5 Quantification of changes in sciatic conduction measured through CMAP distal to the application of the PAR-1 agonists thrombin and SFLLRNPNDKYEPF as described in the 'Methods' section. The X symbols connected by the bold line represent the controls (treated with NaCl 0.9%; $n = 5$) to which all the other groups were compared by statistical analysis at the 60 min time point. The solid symbols connected by straight lines represent mean ± SEM of CMAPs after application of thrombin 10 U/ml (solid squares, $n = 3$, $P = 0.4$), 100 U/ml (solid triangles, $n = 3$, $P = 0.001$) and 200 U/ml (solid diamonds, $n = 3$, $P = 0.0001$). The empty circle symbols connected by dashed lines represent the mean ± SEM of CMAPs after application of thrombin (100 U/ml) together the thrombin inhibitor PPACK (500 μM) $n = 2$ (compared to controls $P = 0.215$, compared to thrombin 100 U/ml $P = 0.05$). The empty symbols connected by dotted lines represent mean ± SEM of CMAPs after application of the PAR-1 agonist SFLLRNPNDKYEPF 150 μM (triangles, $n = 2$, $P = 0.001$) and 300 μM (squares, $n = 2$, $P = 0.001$).

compared to controls ($n = 5$) is presented in Fig. 5. As can be seen, there was a dose-dependent reduction of the CMAPs by thrombin. Exposure of the nerve for 60 min to a high concentration of thrombin, 200 U/ml, resulted in an 80% reduction of CMAP. In contrast, thrombin 10 U/ml or thrombin 100 U/ml applied together with the thrombin inhibitor PPACK did not reduce CMAPs significantly. Figure 5 also presents the quantification of the effects of the PAR-1 agonist SFLLRNPNDKYEPF on nerve conduction. The two concentrations of PAR-1 agonist produced similar results in magnitude and time course to the higher concentrations of thrombin, both producing an 80% reduction in CMAPs 1 h after application. Analysis of variance for the effects of all groups presented in Fig. 5 shows significant effects of treatment ($P < 0.0001$) and interaction of treatment × time ($P < 0.001$). This enabled post hoc analysis comparing the 30 and 60 min time points between the control and each treatment group which revealed significant effects for the high thrombin concentrations, 100 and 200 U/ml and for the agonist treatments, 150 and 300 μM ($P < 0.001$). No significant effects were observed for thrombin applied simultaneously with its inhibitor PPACK or for thrombin 10 U/ml.

Application of trypsin, which activates PAR-2 relatively more than PAR-1, at a concentration of 180 U/ml did not significantly alter CMAPs at any time point ($n = 2$, $P = 0.287$). A higher concentration of trypsin 360 U/ml applied to the nerve caused a 30% reduction in CMAPs after 1 h.

Discussion

The present study demonstrates that PAR-1 is present in sciatic nerves predominantly localized on non-compacted Schwann cell microvilli at the node of Ranvier. Thrombin and a specific agonist peptide produce changes in nerve conduction compatible with a conduction block, presumably by stimulation of PAR-1.

The activation of ERK in response to the specific PAR-1 agonist indicates the presence of functional thrombin receptor in the sciatic nerve. The well-established expression of PAR-1 in the motor neurons (Festoff *et al.*, 2000), and the relatively low levels of PAR-1 expression in the sciatic nerve, which contains mRNA mainly from myelin and connective tissue, would suggest that the receptor is localized predominantly on motor axons. The immunohistological localization of PAR-1 at the node of Ranvier, a critical structure in nerve conduction, indicates however that the primary localization of the receptor is on a highly specific Schwann cell structure at the node. It is interesting to note that we found similar expression of PAR-1 in a primary Schwann cell culture and somewhat higher levels of expression in the optic nerve, brain and spinal cord.

A central finding of the present study is that thrombin has the potential to produce a reversible block in the propagation of action potentials when applied to peripheral nerves. The effect of thrombin was dependent on the protease activity since it was fully blocked by PPACK. Electrophysiologcal effects of a non-specific protease, proteinase K on nerve conduction have been previously reported (Westland and Pollard, 1987) but it is difficult to assess whether PAR-1 pathways are involved in the effects described. The electrophysiological effects of the application of thrombin included diminution of CMAP amplitude. In some experiments stimulation was applied to the nerve distal to the point of thrombin application resulting in normal or slightly increased CMAP (Figs 3 and 4), indicating a focal conduction block. Though *F* waves are variable in latency and amplitude, they seemed diminished by PAR-1 activation when measured in response to proximal (Fig. 3) and even more to distal (Fig. 4) stimulation, a finding that is compatible with alteration in nerve conduction. The present results suggest that electrophysiological effects of thrombin are mediated through PAR-1. After washing off the thrombin or the PAR-1 agonist, conduction was restored after 30 min. The reversible nature of the effect suggests a functional deficit that may be overcome once receptor activation is terminated. The slower onset of action and probably also

Downloaded from brain.oxfordjournals.org at Wix Library on July 31, 2011

recovery from thrombin may be due to its slower diffusion and the fact that it activates the receptor by irreversible cleavage. PAR-1 is shut off by phosphorylation, uncoupled from signalling after activation and then delivered to lysosomes for degradation (Coughlin, 2000). Although high doses of thrombin and the PAR-1 agonists blocked conduction it is interesting to note that during exposure of the nerve to the lowest concentration of thrombin (10 U/ml) or during washing thrombin and the agonist off the nerve, CMAP responses tended to be higher than at baseline. This trend raises the speculative possibility that low levels of PAR-1 activation may augment nerve conduction.

The localization of functional PARs on peripheral nerve has not previously been described. Their expression in motor neuron cell bodies in the spinal cord (Festoff *et al.*, 2000) or sensory neuron cell bodies in the dorsal root ganglia (DRG) (Zhu *et al.*, 2005) and neuromuscular junction [probably on Schwann cells (Lanuza *et al.*, 2007)] are well established but physiological effects on the sciatic nerve are most likely explained by the presence of functional receptors in the nerve itself. The results indicate for the first time an acute electrophysiological effect of PAR-1 activation on motor neurons. Such effects have been described in detail on sensory neurons, especially those involved in mediating nociceptor function and itch and the functional effects of PAR-1 on motor neurons are in line with some of the data from sensory neurons. Although PAR 1–4 are present in the DRG (Zhu *et al.*, 2005), only PAR 1–3 are found on neurons and the predominant receptor which activates nociception in the PNS is PAR-2 (Steinhoff *et al.*, 2003; Kawao *et al.*, 2004). Specificity of PAR activation in disease may depend on a number of factors: Enzyme specificity may be determined by the type of inflammatory cell infiltrate, tryptase would be expected to be increased in diseases in which there is eosinophilia such as Churg–Straus. Acute lesions may differ from chronic lesions in the distribution of PAR receptors.

The exact pathophysiology of conduction block in PNS disease is not known. It is a common feature of demyelinating diseases, especially those of an inflammatory nature (Harvey and Pollard, 1992). Our present findings offer novel anatomical and physiological substrates for the pathogenesis of conduction block. The major anatomical implication of the present findings is that a significant conduction block can be induced through the specific non-compacted myelin microvilli at the node of Ranvier. It is relevant to note that anti-ganglioside antibodies, which are implicated in causing the electrophysiological effects of GBS, are deposited in the area of the node and the adjacent myelin (Santoro *et al.*, 1990; Thomas *et al.*, 1991) and that the gangliosides targeted by these antibodies are also specifically localized to the node of Ranvier and nodal (abaxonal) myelin (Sheikh *et al.*, 1999; Moran *et al.*, 2005). Our findings regarding the induction of conduction block by activation of a receptor specifically localized to the non-compacted myelin microvilli link this structure to nerve conduction abnormalities in diseases such as GBS and anti-GM1 neuropathies. It is assumed that the chain of events leading to conduction block may begin by activation of the Schwann microvilli followed by calcium influx (Yang, 1997) and the secretion of substances which then act on the axon disrupting the propagation of the action potential. This relatively complex set of events may explain the difficulty in determining the role of anti-ganglioside antibodies in causing conduction block (Paparounas *et al.*, 1999). There is currently much interest in the role of glia in modulating neuronal function both at the synapse and at the nodes of Ranvier (Haydon and Carmignoto, 2006; Rousse and Robitaille, 2006). Schwann cells mediate this type of interaction in the PNS while a subgroup of astrocytes do this in the CNS. In order to produce conduction block the stimulation of the PAR-1 receptor on the glial Schwann cell is presumed to influence the interaction of this cell with the neuronal axon and that several mechanisms of such interaction are already known and relevant to the present findings. Known mediators of such glia-neuron cross-talk include glutamate, D-serine and purinergic neurotransmitters (Haydon and Carmignoto, 2006; Rousse and Robitaille, 2006). Further evaluation of the cascade of events following PAR-1 activation in Schwann cells will provide a better understanding of this newly emerging field.

The present findings may be relevant to a number of pathological processes affecting peripheral nerves. States in which peripheral nerve is affected by vascular disease, such as ischaemic neuropathy and vasculitis, are associated with thrombus formation. The thrombin concentrations used in our experiments are in same range as in the serum from coagulated blood [50–100 U/ml (Kumar and Chapman, 2007)] and active thrombin concentrations have not been documented in ischemic or inflamed nerve. It is well established that thrombin is a powerful stimulator of brain endothelial cells (Aronovich *et al.*, 2005) which are the major components of the blood–brain and blood–nerve barriers (BBB and BNB). High levels of thrombin within blood vessels in the nerve and brain would be expected to critically affect endothelial cells causing a breakdown of the BBB and BNB and thus allowing active thrombin to gain access to nerve tissue. In such states conduction is often blocked reversibly and the elevated levels of thrombin in the nerve may offer an alternative explanation for this in addition to nerve dysfunction induced by ischaemia. The present findings may also be relevant to situations in the CNS in which tracts are exposed to high levels of thrombin. These include vascular disease such as both haemorrhage and ischaemia (Lee *et al.*, 1996) and CNS inflammatory diseases such as multiple sclerosis (Koh *et al.*, 1992). This hypothesis suggests the therapeutic use of thrombin antagonists and this may be particularly relevant for the emerging group of small thrombin inhibitor molecules which may penetrate better into nerve tissue. Certain of

Downloaded from brain.oxfordjournals.org at Wix Library on July 31, 2011

these diseases may also be potentially amenable to treatment with PAR-1 antagonists.

Acknowledgements

We thank Dr Leonid Mitelman for his excellent technical work on obtaining the confocal microscope images.

References

Aronovich R, Gurwitz D, Kloog Y, Chapman J. Antiphospholipid antibodies, thrombin and LPS activate brain endothelial cells and Ras-dependent pathways through distinct mechanisms. Immunobiology 2005; 210: 781–8.

Bar-Shavit R, Hruska K, Kahn A, Wilner G. Hormone-like activity of human thrombin. Ann N Y Acad Sci 1986; 485: 335–48.

Beilin O, Karussis D, Korczyn A, Gurwitz D, Aronovich R, Hantai D, et al. Increased thrombin inhibition in experimental autoimmune encephalomyelitis. J Neurosci Res 2005; 79: 531–9.

Berger AR, Logigian EL, Shahani BT. Reversible proximal conduction block underlies rapid recovery in Guillain-Barre syndrome. Muscle Nerve 1988; 11: 1039–42.

Brinkmeier H, Aulkemeyer P, Wollinsky KH, Rudel R. An endogenous pentapeptide acting as a sodium channel blocker in inflammatory autoimmune disorders of the central nervous system. Nat Med 2000; 6: 808–11.

Cicala C, Cirino G. Linkage between inflammation and coagulation: an update on the molecular basis of the crosstalk. Life Sci 1998; 62: 1817–24.

Clark D. Guide for the care and use of laboratory animals. Washington, DC: National Academy Press; 1996.

Coughlin S. Thrombin signalling and protease activated receptors. Nature 2000; 407: 258–64.

Cunningham D, Donovan F. Regulation of neurons and astrocytes by thrombin and protease nexin-1. Adv Exp Med Biol 1997; 425: 67–75.

Dery O, Corvera C, Steinhoff M, Bunnett N. Proteinase activated receptors: novel mechanisms of signaling by serine proteases. Am J Physiol 1998; 274: c1429–52.

Eshed Y, Feinberg K, Poliak S, Sabanay H, Sarig-Nadir O, Spiegel I, et al. Gliomedin mediates Schwann cell-axon interaction and the molecular assembly of the nodes of Ranvier. Neuron 2005; 47: 215–29.

Esmon C. Role of coagulation inhibitors in inflammation. Thromb Haemost 2001; 86: 51–6.

Festoff BW, D'Andrea MR, Citron BA, Salcedo RM, Smirnova IV, Andrade-Gordon P. Motor neuron cell death in wobbler mutant mice follows overexpression of the G-protein-coupled, protease-activated receptor for thrombin. Mol Med 2000; 6: 410–29.

Friedmann I, Faber-Elman A, Yoles E, Schwartz M. Injury-induced gelatinase and thrombin-like activities in regenerating and nonregenerating nervous systems. Faseb J 1999; 13: 533–43.

Gurwitz D, Cunningham D. Thrombin modulates and reverses neuroblastoma neurite outgrowth. Proc Natl Acad Sci 1988; 85: 3440–4.

Harvey G, Pollard J. Patterns of conduction impairment in experimental allergic neuritis. An electrophysiolgical and histological study. J Neurol Neurosurg Psychiatry 1992; 55: 909–15.

Harvey GK, Toyka KV, Zielasek J, Kiefer R, Simonis C, Hartung HP. Failure of anti-GM1 IgG or IgM to induce conduction block following intraneural transfer. Muscle Nerve 1995; 18: 388–94.

Haydon PG, Carmignoto G. Astrocyte control of synaptic transmission and neurovascular coupling. Physiol Rev 2006; 86: 1009–31.

Hirota N, Kaji R, Bostock H, Shindo K, Kawasaki T, Mizutani K, et al. The physiological effect of anti-GM1 antibodies on saltatory conduction and transmembrane currents in single motor axons. Brain 1997; 120 (Pt 12): 2159–69.

Hughes RA, Hadden RD, Gregson NA, Smith KJ. Pathogenesis of Guillain-Barre syndrome. J Neuroimmunol 1999; 100: 74–97.

Inaba Y, Ichikawa M, Inoue A, Itoh M, Kyogashima M, Sekiguchi Y, et al. Plasma thrombin-antithrombin III complex is associated with the severity of experimental autoimmune encephalomyelitis. J Neurol Sci 2001; 185: 89–93.

Kafri M, Drory VE, Wang N, Rabinowitz R, Korczyn AD, Chapman J. Assessment of experimental autoimmune neuritis in the rat by electrophysiology of the tail nerve. Muscle Nerve 2002; 25: 51–7.

Kawao N, Ikeda H, Kitano T, Kuroda R, Sekiguchi F, Kataoka K, et al. Modulation of capsaicin-evoked visceral pain and referred hyperalgesia by protease-activated receptors 1 and 2. J Pharmacol Sci 2004; 94: 277–85.

Koh C, Gauses J, Paterson P. Concordance and localization of maximal vascular permeability change and fibrin deposition in the central neuraxis of Lewis rats with cell-transferred experimental allergic encephalomyelitis. Brain Res 1992; 302: 347–55.

Kumar V, Chapman JR. Whole blood thrombin: development of a process for intra-operative production of human thrombin. J Extra Corpor Technol 2007; 39: 18–23.

Laemmli U. Cleavage of structural proteins during the assembly of the head of bacteriophage T4. Nature 1970; 227: 680–5.

Lanuza MA, Besalduch N, Garcia N, Sabate M, Santafe MM, Tomas J. Plastic-embedded semithin cross-sections as a tool for high-resolution immunofluorescence analysis of the neuromuscular junction molecules: Specific cellular location of protease-activated receptor-1. J Neurosci Res 2007; 85: 748–56.

Lee K, Colon G, Betz A, Keep R, Kim S, Hoff J. Edema from intracerebral hemorrhage: the role of thrombin. J Neurosurg 1996; 84: 91–6.

Luo W, Wang Y, Reiser G. Two types of protease-activated receptors (PAR-1 and PAR-2) mediate calcium signaling in rat retinal ganglion cells RGC-5. Brain Res 2005; 1047: 159–67.

Moran AP, Annuk H, Prendergast MM. Antibodies induced by ganglioside-mimicking Campylobacter jejuni lipooligosaccharides recognise epitopes at the nodes of Ranvier. J Neuroimmunol 2005; 165: 179–85.

Narita M, Usui A, Niikura K, Nozaki H, Khotib J, Nagumo Y, et al. Protease-activated receptor-1 and platelet-derived growth factor in spinal cord neurons are implicated in neuropathic pain after nerve injury. J Neurosci 2005; 25: 10000–9.

Paparounas K, O'Hanlon GM, O'Leary CP, Rowan EG, Willison HJ. Anti-ganglioside antibodies can bind peripheral nerve nodes of Ranvier and activate the complement cascade without inducing acute conduction block in vitro. Brain 1999; 122 (Pt 5): 807–16.

Poliak S, Gollan L, Martinez R, Custer A, Einheber S, Salzer JL, et al. Caspr2, a new member of the neurexin superfamily, is localized at the juxtaparanodes of myelinated axons and associates with K+ channels. Neuron 1999; 24: 1037–47.

Rasband MN, Trimmer JS, Peles E, Levinson SR, Shrager P. K+ channel distribution and clustering in developing and hypomyelinated axons of the optic nerve. J Neurocytol 1999; 28: 319–31.

Ropper AH, Wijdicks EF, Shahani BT. Electrodiagnostic abnormalities in 113 consecutive patients with Guillain-Barre syndrome. Arch Neurol 1990; 47: 881–7.

Rousse I, Robitaille R. Calcium signaling in Schwann cells at synaptic and extra-synaptic sites: active glial modulation of neuronal activity. Glia 2006; 54: 691–9.

Santoro M, Thomas FP, Fink ME, Lange DJ, Uncini A, Wadia NH, et al. IgM deposits at nodes of Ranvier in a patient with amyotrophic lateral sclerosis, anti-GM1 antibodies, and multifocal motor conduction block. Ann Neurol 1990; 28: 373–7.

Schmidlin F, Bunnett N. Protease-activated receptors: how proteases signal to cells. Curr Opin Pharmacol 2001; 1: 575–82.

Sheikh KA, Deerinck TJ, Ellisman MH, Griffin JW. The distribution of ganglioside-like moieties in peripheral nerves. Brain 1999; 122 (Pt 3): 449–60.

Spiegel I, Adamsky K, Eshed Y, Milo R, Sabanay H, Sarig-Nadir O, et al. A central role for Necl4 (SynCAM4) in Schwann cell-axon interaction and myelination. Nat Neurosci 2007; 10: 861–9.

Downloaded from brain.oxfordjournals.org at Wix Library on July 31, 2011

Steinhoff M, Neisius U, Ikoma A, Fartasch M, Heyer G, Skov PS, et al. Proteinase-activated receptor-2 mediates itch: a novel pathway for pruritus in human skin. J Neurosci 2003; 23: 6176–80.

Thomas FP, Trojaborg W, Nagy C, Santoro M, Sadiq SA, Latov N, et al. Experimental autoimmune neuropathy with anti-GM1 antibodies and immunoglobulin deposits at the nodes of Ranvier. Acta Neuropathol (Berl) 1991; 82: 378–83.

Towbin H, Staehelin T, Gordon J. Electrophoretic transfer of proteins from polyacrylamide gels to nitrocellulose sheets: procedure and some application. Proc Natl Acad Sci USA 1979; 76: 4350–4.

Turnell AS, Brant DP, Brown GR, Finney M, Gallimore PH, Kirk CJ, et al. Regulation of neurite outgrowth from differentiated human neuro-epithelial cells: a comparison of the activities of prothrombin and thrombin. Biochem J 1995; 308 (Pt 3): 965–73.

Vergnolle N, Ferazzini M, D'Andrea MR, Buddenkotte J, Steinhoff M. Proteinase-activated receptors: novel signals for peripheral nerves. Trends Neurosci 2003; 26: 496–500.

Vu T, Hung D, Wheaton V, Goughlin S. Molecular cloning of a functional thrombin receptor reveals a novel proteolytic mechanism of receptor activation. Cell 1991; 64: 1057–68.

Westland K, Pollard J. Proteinase induce demyelination an electrophysiological and histological study. J Neurol Sci 1987; 82: 41–53.

Yang Y. Thrombin receptor on rat primary hippcampal neurons:coupled calcium and cAMP responses. Brain Res 1997; 761: 11–8.

Zhu WJ, Yamanaka H, Obata K, Dai Y, Kobayashi K, Kozai T, et al. Expression of mRNA for four subtypes of the proteinase-activated receptor in rat dorsal root ganglia. Brain Res 2005; 1041: 205–11.

Downloaded from brain.oxfordjournals.org at Wix Library on July 31, 2011